Self-Similar watermarks for counterfeiting geometrical attacks

V. Solachidis[1], S. Tsekeridou[2], S. Nikolopoulos[1] and I. Pitas[1]

[1]Department of Informatics, Aristotle University of Thessaloniki
Box 451, Thessaloniki 54124, Greece
e-mail: {vasilis, nikolopo, pitas}@aiia.csd.auth.gr
[2]Electrical & Computer Engineering Dept. Democritus Univ. of Thrace
Xanthi 67100, Greece
e-mail: tsekerid@ee.duth.gr

Abstract. This manuscript introduces the concept of self similar watermarks for the purpose of counterfeiting geometrical attacks on copyright protected still images. Geometrical transformations result in the de-synchronization of watermark detection mechanisms enforcing the adoption of exhaustive search strategies for optimizing the algorithm's efficiency. The self-similar structure attained by the presented watermarks reduces the search ranges and enhances the detection performance by accelerating the overall procedure and minimizing the false detection probability. Various embedding domains (DFT, DWT) were utilized for hiding the watermark information while the presented schemes do not require the original image during detection. Self-similar watermarks prove rather robust against many kinds of attacks, such as linear and non linear filtering, jpeg compression, scaling, cropping and rotation, especially when combined with a robust transform domain.

Introduction

Intellectual Property Rights constitutes a challenging problem attracting great interest from both the legislative and technological community. Watermarking emerged as a promising technological solution for solving the problem of protecting the copyrights of multimedia data. The idea to imperceptibly convey information about the copyright owner within the digital content of a protected work seems the only viable solution in a completely loose and open environment like Internet. Watermarking techniques aim at encoding copyright holder identification data directly into the content of digital artworks (images, audio, video etc), in the form of statistical undetectable and perceptually transparent signals. The credibility of such techniques in resolving disputes between the legitimate copyright owner and an adversary lies on the watermark's ability to withstand both hostile and unintentional data manipulations.

Several watermarking methods have been proposed in the literature. An overview can be found in [1-3]. The major flaw of most existing watermarking methods is their inability to cope with the de-synchronization introduced when applying geometrical transformations to the image. In order for the detection mechanism to successfully detect the de-synchronized watermark, all possible combinations of geometric distortions (scaling, rotation, cropping, etc.) that might have been applied on the host image should be considered. In other words, the detector is obliged to perform an exhaustive search of the solution space and initiate brute force algorithms for achieving the necessary synchronization. However, the rather prohibiting computational complexity of the aforementioned approach and the dramatic increase of false detection probability render exhaustive search an inefficient solution. The problem is addressed in the literature by several researchers that try to optimize the procedure and deal with geometrical attacks more efficiently. The proposed solutions can be categorized as follows:

- Utilization of salient image features as anchor points for watermark embedding and detection
- Use of watermarks that, due to their spatial structure and embedding domain, are invariant to geometrical transformations
- Use of watermarks with a structure that results in a significant reduction of the possible distorted space that should be examined during detection.

The watermarks presented in this manuscript belong to the second and third category. The self similar structure of the constructed watermarks is accomplished by the symmetric replication of a base watermark with respect to a cartesian grid and a ring shaped pattern.

The efficiency of self similar watermarks has been tested in various domains (DFT, DWT) by implementing the corresponding watermarking algorithms and evaluating their performance. Both

algorithms are blind and utilize a correlation function and a decision threshold for detecting the watermark signal.

Watermark Generation

The major drawback of integrating an exhaustive search strategy for counterfeiting geometrical attacks within a watermarking system is that extensive search ranges have to be defined and examined. The impact of such strategy affects both the overall computational complexity of the system as well as the false detection probability. Few attempts are reported to successfully deal with certain geometric transformations [4,5]. The concept of utilizing watermarks that possess self-similar structure is to reduce the search ranges in case of cropping, rotating and scaling and thus minimize computational effort. The notion of symmetry is the key attribute that every watermark must feature, in order for the detection mechanism to accelerate its performance.

Among the basic features of a robust watermarking scheme is its immunity to rotation transformations. Therefore, a self-similar circular symmetric watermark must be constructed attaining special attributes with respect to a ring shaped pattern [4]. The replication of a base watermark along a circular orientation produces a symmetry that allows the detection mechanism to reduce the search ranges and thus, optimize the procedure.

Let $W_M(r,\theta)$ be a 2-D ring shaped bipolar sequence taking values 1 or -1. The mean value of the sequence is zero. This sequence can be expressed in a polar coordinate system as follows:

$$W(r,\theta)=\begin{cases} 0, \; if \; r < R_1 \quad or \quad r > R_2 \\ \pm 1, \quad if \quad R_1 < r < R_2 \end{cases}$$

where $r=\sqrt{n_1^2+n_2^2}$ with (n_1,n_2) representing the spatial coordinates and $\theta=\arctan\left(\frac{n_2}{n_1}\right)$, R_1 and R_2 are the minimum and maximum radii that define the watermark's ring-like support and α is a factor that determines the strength of the watermark. Additionally, the ring is divided in *S* sectors having an extent of $\frac{360^o}{s}$. This circular symmetric structure forms the basis for the construction of self similar watermarks used by the presented methods. However, since each method integrates circular symmetry in a different manner additional details regarding watermark generation will be presented separately.

Watermarking Embedding & Detection

Discrete Fourier Transform Domain

DFT (Discrete Fourier Transform) represents the frequency domain of the image and is the preferred embedding domain of many advanced watermarking methods mainly because of the high level of robustness attained against common signal processing attacks. Due to certain properties that DFT holds with respect to rotation and scaling, embedding the watermark signal to the frequency domain constitutes a suitable choice for achieving geometric immunity [10].

Let $I(n_1,n_2)$ be a grayscale $N\times N$ image. The Fourier transform of *I* is:

$$I(k_1,k_2)=\sum_{n_1=0}^{N-1}\sum_{n_2=0}^{N-1}I(n_1,n_2)e^{-j2\pi n_1k_1/N-j2\pi n_2k_2/N}$$

By assuming that the zero frequency term *I(0,0)* is located at the center of the transformation domain, the region in which the watermark is embedded should be a ring covering the middle frequencies. Let $M(k_1,k_2)=|I(k_1,k_2)|$ be the magnitude and $P(k_1,k_2)$ the phase of the Fourier transform of $I(n_1,n_2)$. Let also $W(k_1,k_2)$ be the watermark, $M'(k_1,k_2)$ the modified Fourier magnitude and $I'(k_1,k_2)$ the Fourier transform of the watermarked image. The watermark consists of a 2-D ring shaped bipolar sequence, as the one mentioned above, with the additional feature that all sectors are identical.

The ring shaped watermark consists of several sub-rings. Each sub ring is a scaled version (by a factor of 2) of its inward neighbor sub-rings. Thus, the thickness of its ring is twice the thickness of each inward neighbor. A representation of the watermark can be seen in Figure 1. The pattern of image Lenna is used to exemplify the self-similar structure of the watermark.

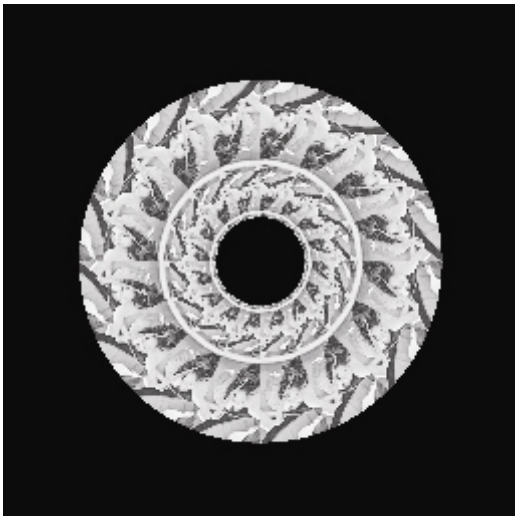

Fig. 1. Example of a self-similar watermark

The Fourier magnitude M' of the watermarked image is given by:

$$M'(k_1,k_2)=M(k_1,k_2)+aW(k_1,k_2)$$

If the magnitude becomes negative, it is rounded to 0. The watermarked image $I'(n_1,n_2)$ is given by the inverse DFT:

$$I'(n_1,n_2)=IDFT(I'(k_1,k_2))$$
$$I'(k_1,k_2)=M'(k_1,k_2)e^{P(k_1,k_2)}$$

Watermark detection is performed by calculating the normalized correlation between the host image and a specified watermark and comparing the result with a predefined threshold. Let $I''(k_1,k_2)$ be the DFT of a possible watermarked image and $M''(k_1,k_2)$ its magnitude. The correlation *c* between M'' and the watermark W derives from the following equation:

$$c=\sum_{i=1}^{N}\sum_{j=1}^{N}W(k_1,k_2)M''(k_1,k_2)$$

If image I is watermarked with W', $W \neq W'$, then the correlation *c* is given by:

$$c = \sum_{i=1}^{N}\sum_{j=1}^{N}(W(k_1,k_2)M(k_1,k_2) + aW(k_1,k_2)W'(k_1,k_2))$$

If image I is watermarked with W the correlation *c* is:

$$c = \sum_{i=1}^{N}\sum_{j=1}^{N}(W(k_1,k_2)M(k_1,k_2) + aW^2(k_1,k_2))$$

Assuming that $W(k_1,k_2)$, $M(k_1,k_2)$ are independent and identically distributed random variables and W has zero mean value, the value of *c* is:

$$\mu_c = \begin{cases} \pi(R_2^2 - R_1^2)\alpha & if\ W = W' \\ 0 & if\ W \neq W' \\ 0 & if\ watermark\ is\ not\ present \end{cases}$$

The normalized correlator output $c' = \dfrac{c}{\mu_c}$ is used for deciding upon the watermark's existence. The mean value of the normalized correlator c' should be 0 for images that are not watermarked or watermarked with another watermark (W') and 1 for watermarked images (with right watermark).

The detection rule could be of the form:

I' is watermarked by *W* if $c \geq T$

I' is not watermarked by *W* if $c < T$

where T is an appropriate selected threshold.

Discrete Wavelet Transform Domain [9]

Wavelet decomposition formulates a suitable framework for time/frequency, spatial/frequency analysis of signals and has gained significant attention in the field of information hiding. In addition, it provides a multiresolution approach to signal representation which is particularly suited for modeling the HVS. The above considerations render the wavelet domain an ideal candidate for embedding watermarking information, especially in situations where the method's payload requirements are heavy.

The watermarks utilized by the wavelet domain implementation possess slightly different attributes comparing to the DFT case. In particular, instead of using identical elementary signals for covering the sector areas, one common value is uniformly embedded in each circular sector. In other words, all pixels inside a sector for a constant radius are set equal to –α or +α according to a pseudorandom generator initialized by a predefined key. An example of the base watermark, from here on called mother signal, is depicted in Figure 3a.

The next step is to incorporate spatial self-similarity with respect to the cartesian grid. Spatial symmetry is necessary for counterfeiting rescale transformations. The circularly symmetric watermark described above $W_M(n_1,n_2)$ is scaled (using nearest neighbor interpolation) and shifted with respect to its center (*r=0, θ=0)* 3 times, thus allowing possibility of watermark detection for scaling factors ranging in $\left[\frac{1}{8},1\right]$ as shown in Figure 2. The final watermark $W(n_1,n_2)$ is evaluated by:

$$W(n_1,n_2)=\sum_{f=0}^{3}\sum_{i=0}^{2^f-1}\sum_{j=0}^{2^f-1}W_M(2^f n_1+i\left\lceil\frac{R_2}{2^f}\right\rceil 2^f n_2+j\left\lceil\frac{R_2}{2^f}\right\rceil$$

It is evident that the watermark dimensions are $2R_2 \times 2R_2$ and are totally independent of the image size. The parameters that are necessary for the watermark generation and which corresponds to the final key for detection are: $\{k, a, R_1, R_2\}$. The center of the watermark is used as a reference point in the detection phase. An example of the final watermark is given in Figure 3b.

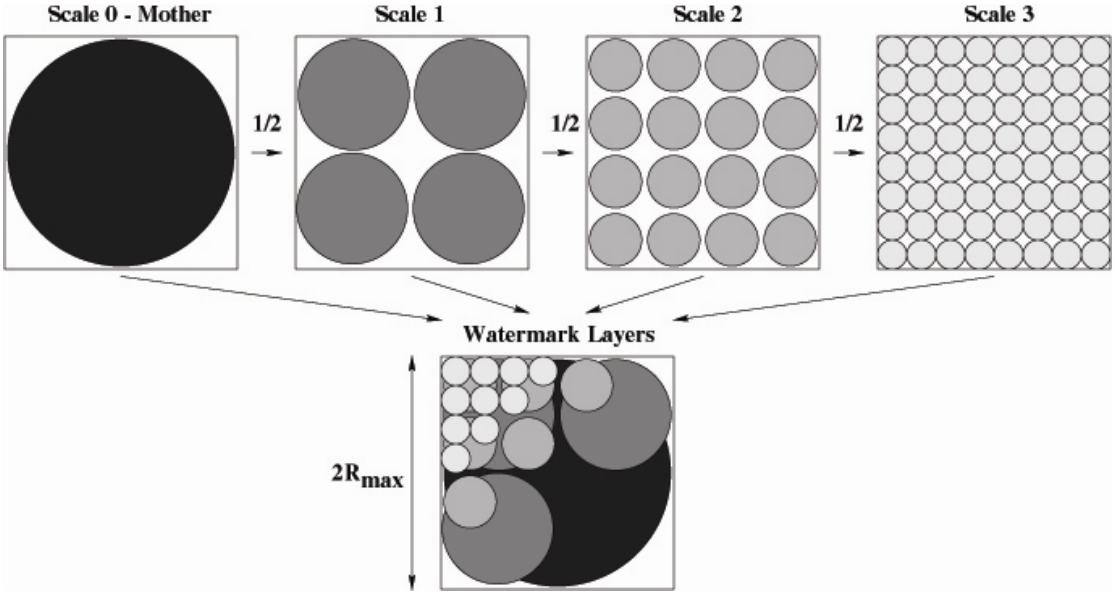

Fig. 2. Illustration of the self-similarity in the watermark generation process

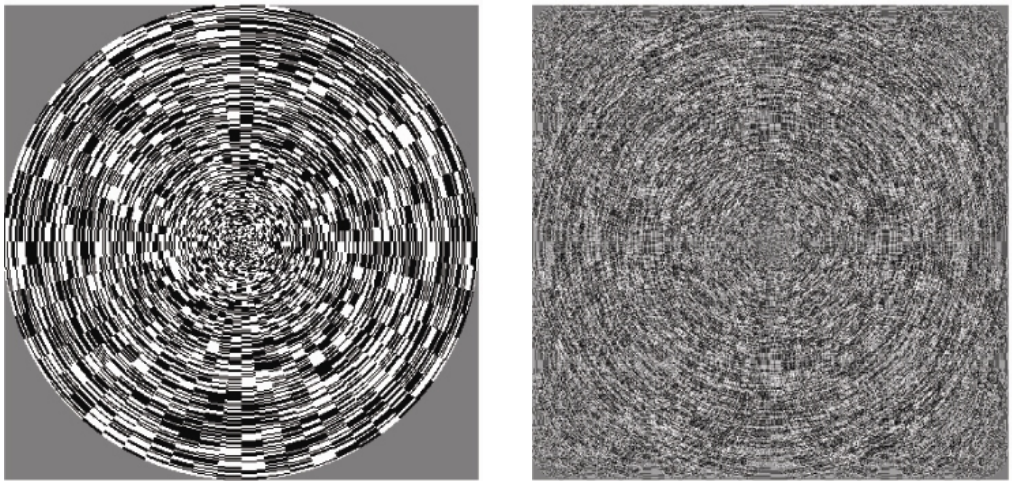

(a) (b)

Fig. 3. Example of a (a) base signal, (b) self-similar watermark

Embedding is performed in the wavelet domain where the watermark is superimposed. The image is decomposed in 4 levels using both the Haar and the Daubechies-4 wavelet basis. $W(n_1,n_2)$ is superimposed on the detail subbands of the 1st and 2nd levels of the decomposed original image $I(n_1,n_2)$ as shown in Figure 4, i.e.:

$$I'_{f_l} = I_{f_l} \otimes W(2^{l-1}n_1, 2^{l-1}n_2), f \in \{LH, HL, HH\},\ l \in \{1,2\}$$

where $\otimes$ is a superposition operator. I_{f_l} and I'_{f_l} stand for the detail subband components of the original and the watermarked image respectively, f for the subband index and l for the level index of the wavelet decomposition, where embedding is performed. It should be noted that the watermark size must be smaller or equal to half of the size of the image to be watermarked. If it is smaller, it is added in the center of the detail subband component. Embedding in the 2nd level requires watermark scaling by 1/2. No embedding is performed to lower DWT levels, since they are considered unreliable, due to the smaller number of pixels that are watermarked. After watermark superposition, inverse DWT is performed to obtain the watermarked image $I'(n_1, n_2)$. Due to the inherent spatial localization and frequency spread of DWT, implicit visual masking is accomplished leading to watermark perceptual invisibility. Embedding is also performed in the 2nd level of the transform to ensure watermark detection after distortions such as filtering or compression which tend to remove high frequency components of the image (1st level of DWT).

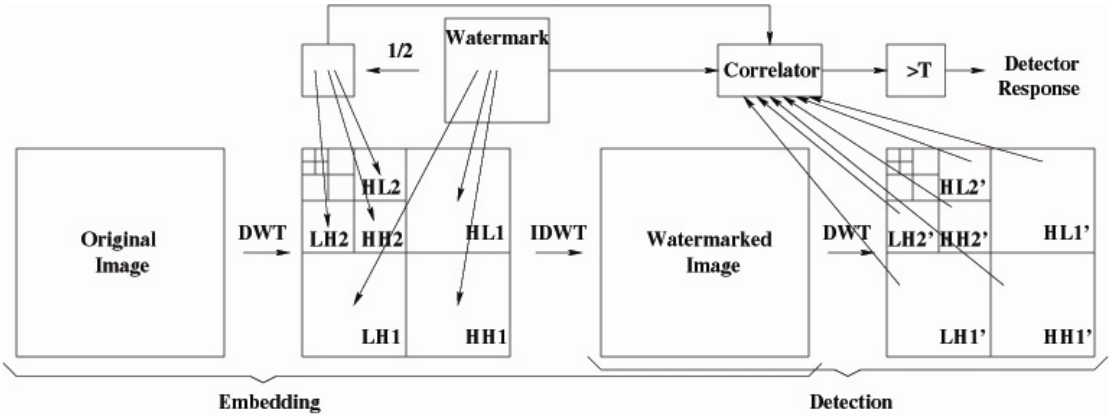

Fig. 4. Presentation of the watermark embedding and detection methods in the wavelet domain

Watermark detection is performed statistically without the use of the original image. Initially, the watermarked image $I'(n_1, n_2)$ is DWT transformed and the correlations between the watermark (or scaled watermark) and the detail subband components of the 1st and 2nd levels are calculated, as shown in Figure 4. Thus, the following normalized correlator is evaluated:

$$\rho(l, f) = \frac{I'_{f_l} \cdot W_{2^{l-1}}}{W_{2^{l-1}} \cdot W_{2^{l-1}}}, \qquad l \in \{1,2\}, \quad f \in \{LH, HL, HH\}$$

for each frequency orientation f (subband component) and for each level l. $\cdot$ denotes inner product. $W_1(n_1, n_2) = W(n_1, n_2)$ and $W_2(n_1, n_2) = W(2n_1, 2n_2)$. Since I'_{f_l} and W are statistically independent, it is obvious that $\rho(l, f)$ will be 1 under watermark presence and 0 under watermark absence. In order to estimate the overall correlator response, average values along each frequency orientation f are initially estimated and then the maximum value over all frequency orientations f is estimated too:

$$\rho = \max_f \left\{ \frac{1}{2} \sum_l \rho(l, f) \right\}$$

Average values along each frequency orientation aid in enhancing the correlation value especially after filtering or compression, where higher levels of the decomposition tend to be more affected. The final correlator response has been chosen as the maximum value of all subbands in order to exploit any strong structure existent in the image (e.g. many vertical edges) where the watermark is better retained.

The correlator function mentioned above works satisfactorily under image distortions such as filtering or compression where spatial supports are not changed. In order to detect the watermark under geometric transformations, the correlator uses scaled and shifted versions of W_M, with respect to its center, instead of W. It is easily proven that, when a watermark exists, its value is 1, and when it does not, its value is 0. It is also easily seen that the search ranges with respect to scaling factors and shifts are much reduced using this correlator and based on the self-similar structure of the watermark. Detection is performed by comparing ρ against a predefined threshold. The latter is estimated under a false alarm probability constraint.

Geometrical Robustness Verification & Simulation Results

DFT based Method

The proposed method is robust to translations, since they do not affect the DFT magnitude. Rotation in the spatial domain causes rotation on the Fourier domain by the same angle [6]. Since the watermark consists of S sectors having identical values, watermark detection is possible even after a rotation $\frac{2k\pi}{s}$ degrees of the watermarked image, where $k = 0,1,2,....,S-1$. Thus, a search for the angles $0,1,2,.....,\frac{2k\pi}{s}-1$ suffices to perform detection for every rotation angle. Rotation and translation invariance is a very useful property mainly because printed, scanned or xeroxed copies of an image might be rotated or translated in comparison with the initial image. The presented method is also robust to rotation around an arbitrary center, since rotation around an arbitrary center is equivalent to rotation around the center of the image translation.

Scaling in the spatial domain causes inverse scaling in the frequency domain $(if \quad f(x_1,x_2) \xrightarrow{DFT} F(k_1,k_2) \quad then \quad f(sx_1,sx_2) \xrightarrow{DFT} \frac{1}{s}F(\frac{k_1}{s},\frac{k_2}{s}))$ [6]. Thus, if $N \times N$ is the size of the initial image and $[R_1,R_2]$ is the size of the watermark ring in the frequency domain, the size of the scaled image is $sN \times sN \quad (s>0)$ and the size of the watermark of the scaled image in the frequency domain remains unaltered. Furthermore, normalized correlation output does not depend on s.

Cropping changes the frequency sampling step. If the size of the initial image is known, the correlation can be performed between the cropped image (in the frequency domain) and the watermark, which should be adapted to the frequency sampling step of the cropped image. If the size of the initial image is not known then the correlation should be performed for many frequency sampling steps.

The method is also robust to combined cropping and scaling. Let I' be an $M' \times N'$ image which is possibly scaled and cropped. The detection algorithm correlates a watermark with a ring shaped segment of the frequency domain of I' whose size is bR_1 (inner radius) and bR_2 (outer radius) for every b $(0 < b < 1)$. For example, if the size of the original image is 512 × 512 and the size of the cropped watermarked image is 400 × 400 then we get a maximum c' for b=0.78125 = 400/512 that manifests the existence of the watermark. However, thanks to the self-similar structure of the watermark a reduction of the search range to $[0.5 < b < 1]$ is possible. Therefore, the number of the different frequency sampling steps where the search should be performed is halved (in our case reduced from 512 to 256). In Figure 5 the normalized correlator output for several frequency sampling steps and rotation angles for a watermarked image that has not been distorted is depicted. The multiple peaks due to the self-similarity of the watermark can be clearly seen.

The presented algorithm was tested on a number of digital images using several different keys. The assessment of the algorithm's overall performance resulted in very encouraging conclusions. We present the percentage of the correlator values that is above the selected threshold. Three thresholds have been chosen, T=0.1, T=0.15 and T=0.2. The probability of false alarm for these thresholds is $4 \cdot 10^{-2}$, $4 \cdot 10^{-3}$ and $2 \cdot 10^{-4}$ respectively. Having set the threshold T, the performance criterion used for comparing the performance of the algorithms under image processing operations was the detection ratio defined as: $P = \frac{N_{\det ect}}{N_{total}}$ where $N_{\det ect}$ is the number of the correctly detected watermarks in the

N_{total} experiments. By fixing the strength parameter α, watermarked images distorted to 30 and 35 *db* SNR were generated.

The experiments proved that the watermark is robust to JPEG compression, scaling, cropping, rotation, histogram equalization, Gaussian noise, median and moving average filtering. It is also robust to the various attacks introduced by StirMark evaluation tool. Furthermore, it is robust to rotation at any angle and to combined cropping/scaling if the search procedure described above is used

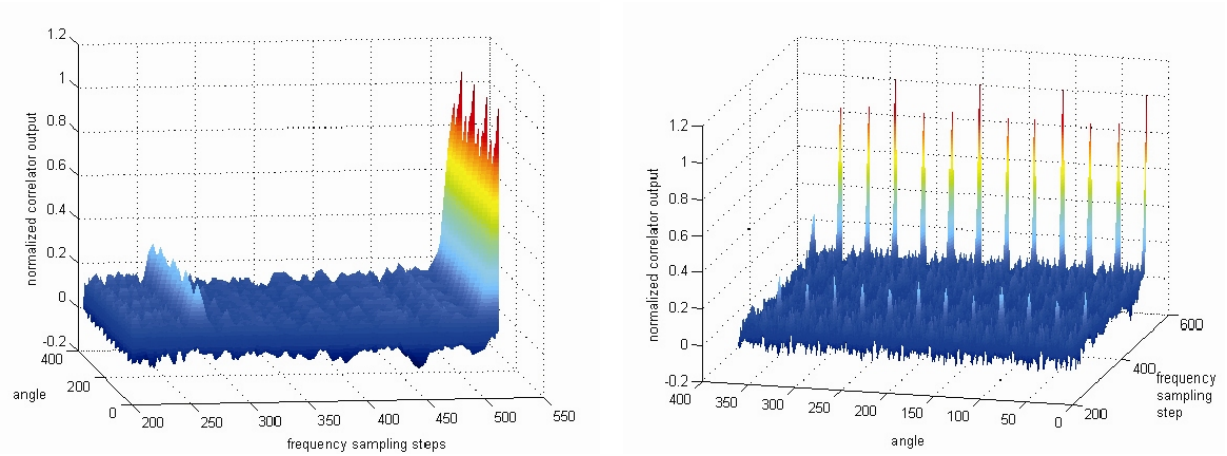

Fig. 5. Normalized correlator output for several frequency steps and rotation angles (two different view angles)

DWT based Method

Five different grayscale images of size 960 × 960 have been used. The embedded watermark power has been varied to produce watermarked images with SNR of 30, 35 and 40dB. The stronger the embedded watermark is, the more visible it tends to be. In order to experimentally prove that different watermarks are uncorrelated to each other, the correlations between a watermark with index 100 and 900 watermarks, differing only in the key parameter k, have been calculated (Figure 6). Figure 7 shows the correlations between the scaled and shifted mother signal and the watermark. These correlations, attained due to the self-similarity, are exploited under geometric distortion cases.

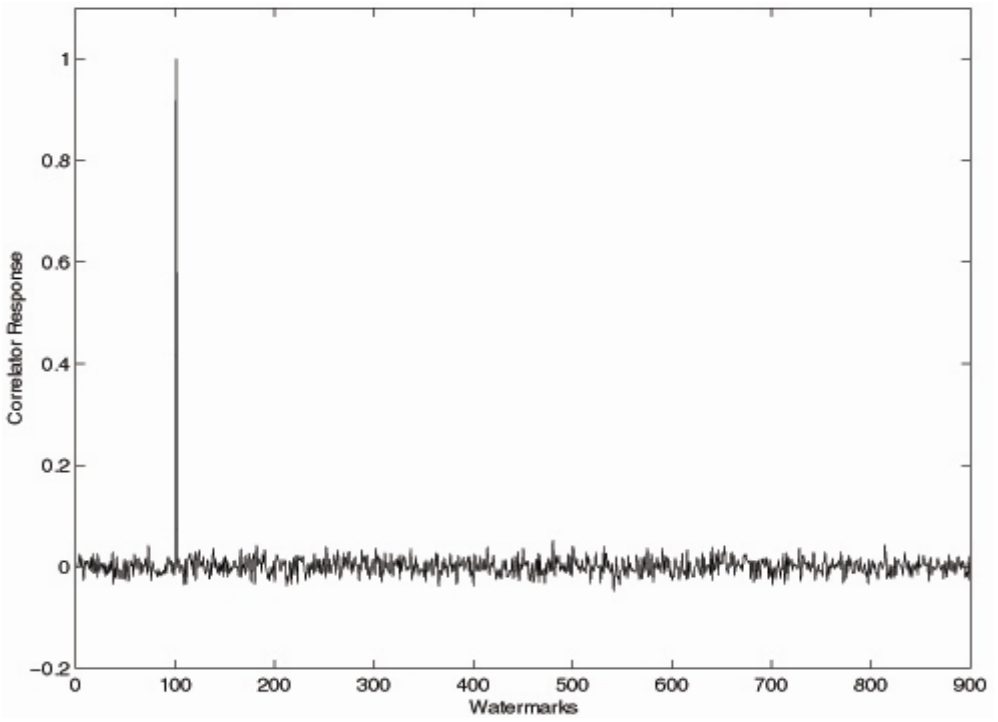

Fig. 6. Correlator response between 900 different watermarks and watermark no 100

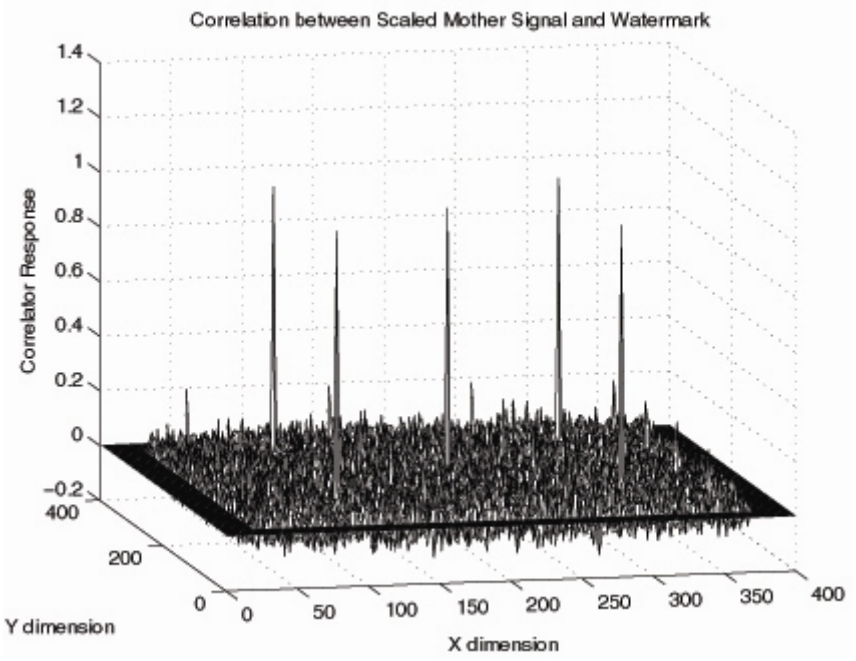

Fig. 7. Correlation between scaled versions of mother signal and watermark

In order to evaluate the detection thresholds for each SNR case, the correlator response for 500 watermarks (5 images, 100 watermarks) has been calculated under watermark presence, absence and use of wrong watermark. Based on their pdfs and for a false alarm probability of 10^{-4}, detection thresholds have been set to: 0.05 when SNR=30 db, 0.085 when SNR = 35 dB and 0.15 when SNR = 40 dB for all distortion cases and for additive embedding. The thresholds for multiplicative embedding are larger since the correlator variance is also bigger, e.g. 0.08 when SNR = 30. Two different wavelet basis have been used in the DWT, the Haar and the Daubechies-4. Detection results using either basis do not deviate greatly. When no distortions are present, the watermark is always detected. Multiple watermarking has also been tested. Five different watermarks have been embedded to a single image

and detection has followed for 100 watermarks including these five ones. The results are illustrated in Figure 8. It is seen that all five watermarks are detected. Linear (mean) and non-linear (median) filtering has also been tested. The detection ratios attained are illustrated in Table 1. The method proves robust against mean and median filtering of size 3 × 3 even when the embedded watermarks are not high-powered. However, for greater size windows, its performance deteriorates.

Table 1. Detection Ratios (%) after the mean and median filtering

SNR	Filter Type			
	Moving Average		Median	
	3 x 3	5 x 5	3 x 3	5 x 5
30	100	92.4	100	100
35	100	16.2	100	98.4
40	99	1	100	34.2

Robustness to JPEG and wavelet compression with different compression ratios has further been studied. Wavelet compression is performed by the SPIHT coder of [7] and the coder of the ATT DjVu Reference Library [8]. Detection results are plotted in Figures 9 and 10. The method proves remarkably robust even for weak watermarks (40dBs) and high compression ratios. Geometric distortions have been also considered. The correlator response is calculated using the mother signal and it's scaled by 1/2 and shifted versions. A detection ratio of 95% has been found after rotation by 2^o without the use of any search range. Rotation by greater angles can also be handled in the way described in [4]. Non-uniform cropping, while preserving the initial image size, has led to 100% detection. The case of non-uniform cropping, leading to a new image size, has also been studied. Search regions for horizontal and vertical shifts are initialized based on the watermark size and structure. Knowledge of the initial image size is not required. It is noted that the watermark size does not depend on the image size. The correlator response after cropping is shown in Figure 12. The peak coordinates additionally inform us about the exact number of cropped rows and columns, with respect to the top-left pixel, from the initial image. Scaling of the watermarked images by a factor of 1.2 has also led to 100% detection. The correlator response is shown in Figure 11. The search range in the scale factor is reduced to [0.5 : 2.0] due to the watermark self-similarity, and peaks appear when the scale factor is 1.2. It is noted that scalings by a factor being a small power of 2 can be directly dealt with. The combined distortion of cropping followed by scaling of the initial image has also been dealt with. Detection is possible in this case too, as Figure 13 shows, where correlations with the scaled by 1/2 mother signal are estimated only in the first top-left quarter of the watermark. In this way, computations are significantly reduced. Search ranges in the scale factor are set to [1.0 : 2.0]. The search ranges for shift values depend on the scale factor and are defined with respect to the scaled watermark size and structure.

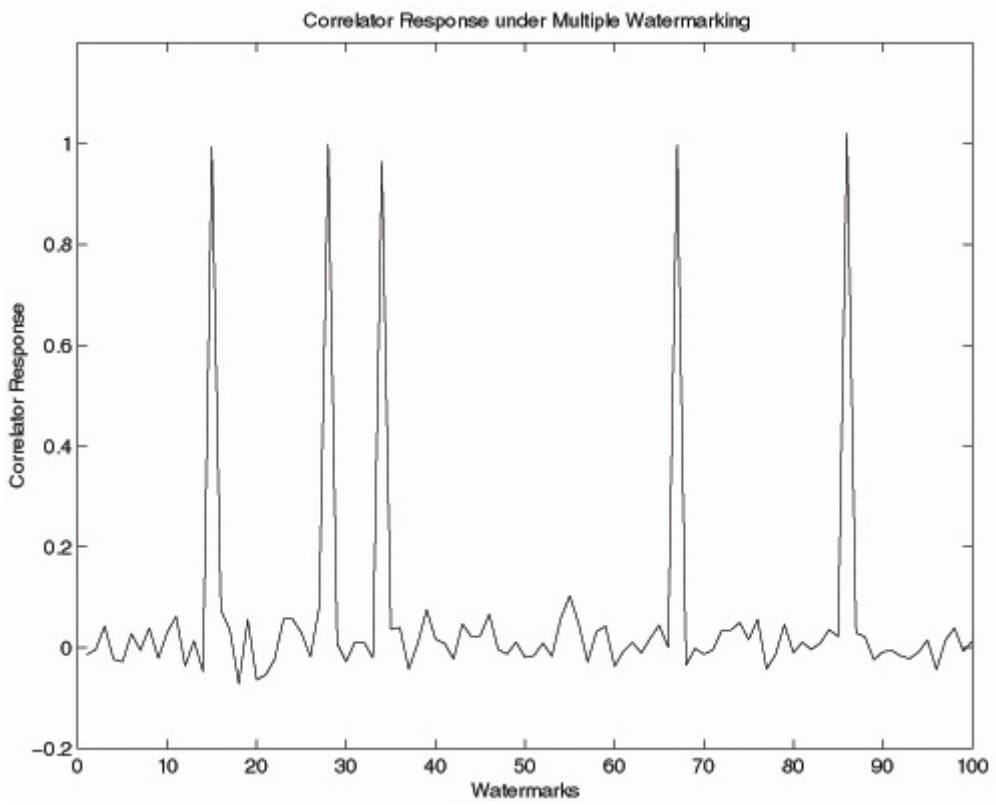

Fig. 8. Correlator output under multiple watermark presence. The correct watermarks are: 15, 28, 34, 67 and 86

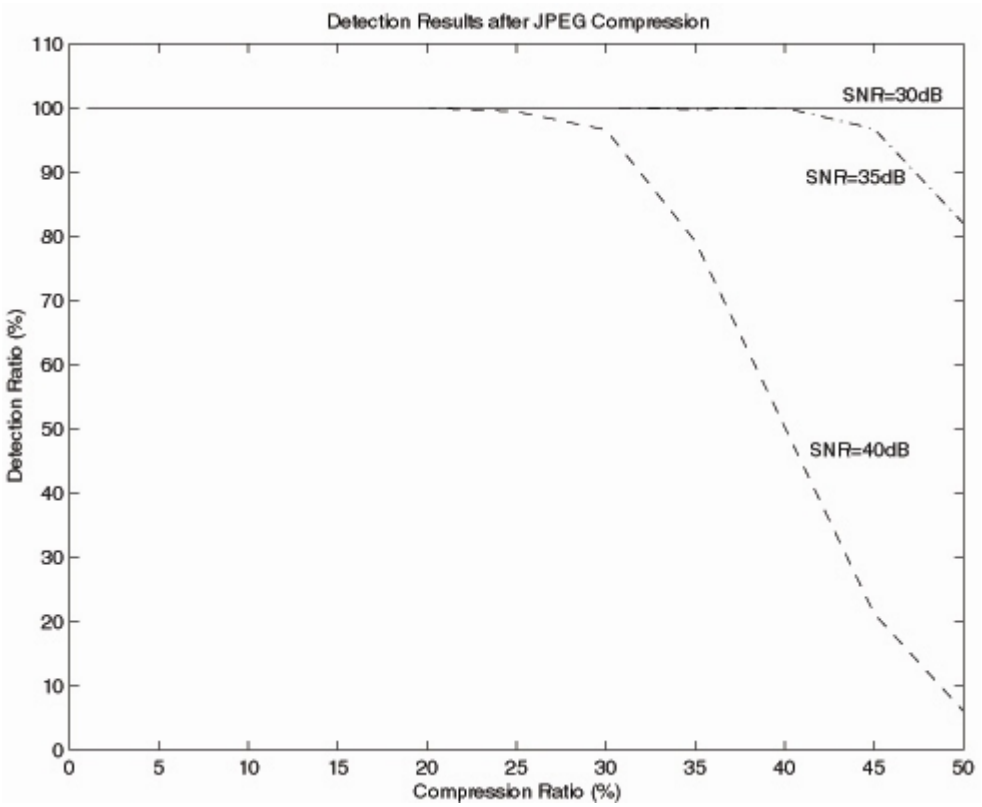

Fig. 9. Watermark resistance to JPEG compression (SNR: 30, 35, 40, dB)

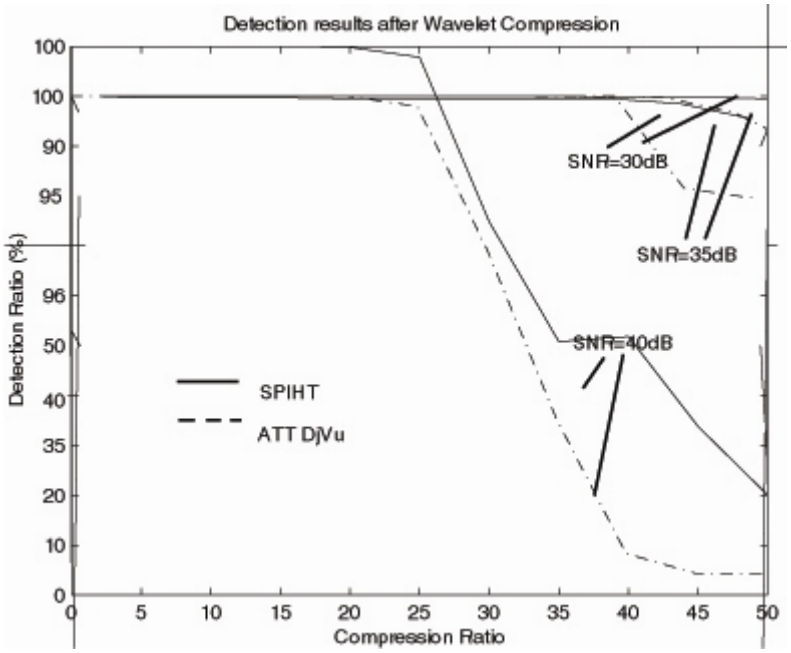

Fig. 10. Watermark resistance to wavelet compression: SPIHT, ATT DjVu (SNR: 30 dB)

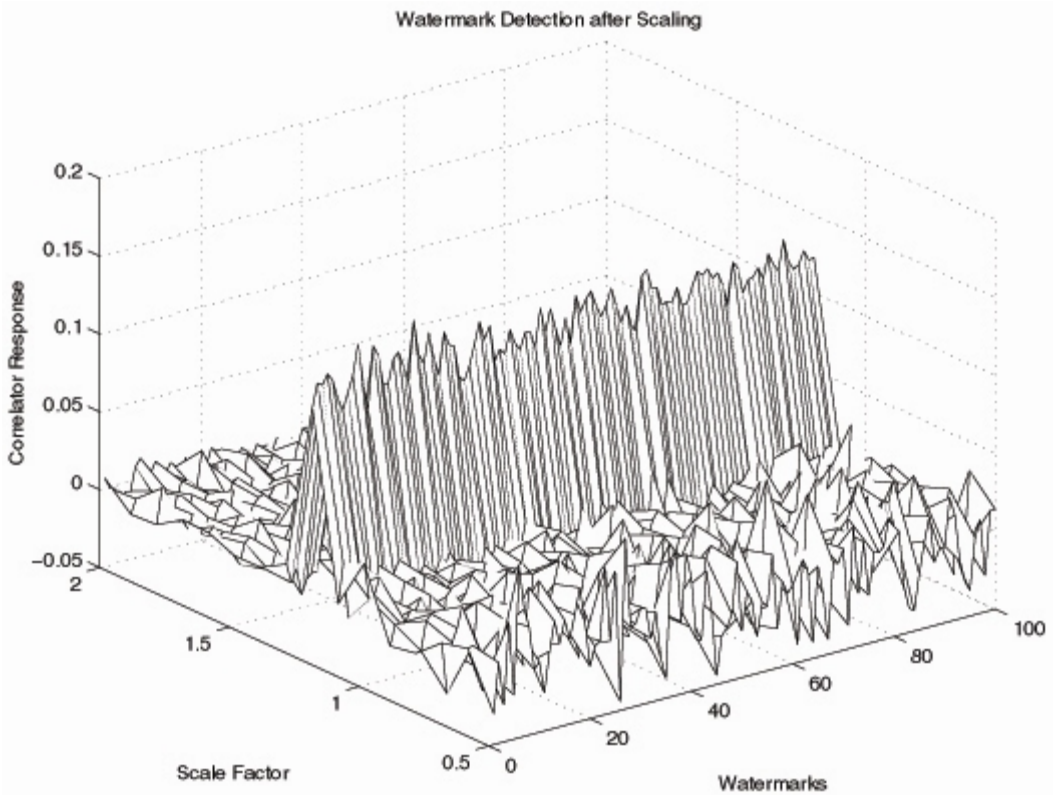

Fig. 11. Corellator response after scaling for 100 different watermarks, scale factor 1.2 (correlation with mother signal)

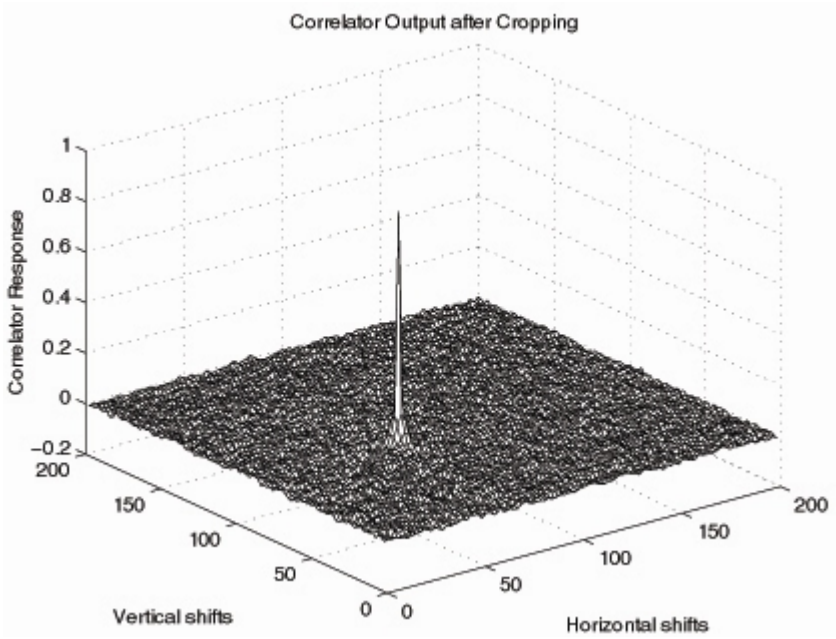

Fig. 12. Corellator response after cropping, cropped region [130:950, 90:930]

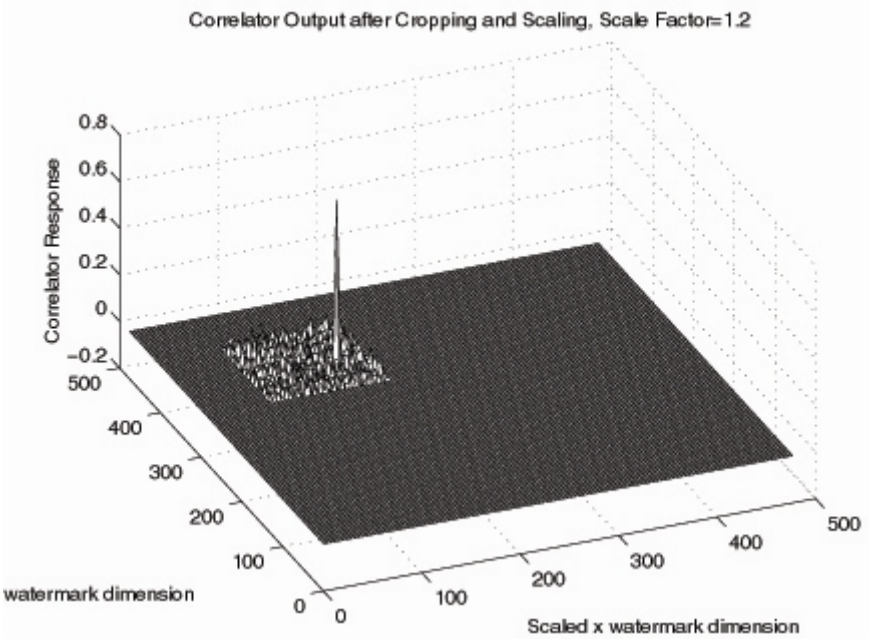

Fig. 13. Corellator response after cropping and scaling, scale factor 1.2, cropped region [40:840, 60:860] (SNR=30dB).

Conclusions

The concept of self similar watermarks for efficient counterfeiting of geometrical transformations has been presented throughout this manuscript. Two different transform embedding domains were utilized for watermark encoding, proving that the benefits of self similar watermarks are independent of the underlying method. Numerous experiments have been conducted using both implementations, and the derived results verified the geometrical immunity achieved by the presented watermarks mainly due

to their self similar structure. Additionally, both methods exhibit increased robustness against filtering, jpeg compression and noise addition. The idea behind self similarity is the reduction of search ranges, balancing between the benefits of exhaustive search and template matching approaches.

References

[1]. F. Hartung and M. Kutter, “Multimedia watermarking techniques,” Proceedings of the IEEE, vol. 87, no. 7, pp. 1079–1107, July 1999.

[2]. M.D. Swanson, M. Kobayashi, and A.H. Tewfik, “Multimedia data embedding and watermarking technologies,” Proceedings of the IEEE, vol. 86, no. 6, pp. 1064–1087, June 1998.

[3]. G. Voyatzis and I. Pitas, “The use of watermarks in the protection of digital multimedia products,” Proceedings of the IEEE, vol. 87, no. 7, pp. 1197–1207, July 1999.

[4]. V. Solachidis and I. Pitas, “Circularly symmetric watermark embedding in 2-d dft domain", in Proc. of ICASPP'99, 15-19 Mar. 1999.

[5]. M. Barni, F. Bartolini, V. Cappellini, A. Lippi, and A. Piva, “A DWT-based technique for spatio frequency masking of digital signatures", in Proc. of SPIE EI'99, vol. 3657, 25-27 Jan. 1999.

[6]. J. O Ruanaidh and T. Pun. “Rotation. scale and translation invariant digital image watermarking”. In Proceedings of ICIP’97 volume I, pages 536-539, Atlanta, USA, October 1997

[7]. A. Said and W.A. Pearlman, “A new, fast and efficient image codec based on set partitioning in hierarchical trees”, IEEE Trans. on CAS for Video Techn., vol. 6, pp. 243-250, Jun. 1996

[8]. “ATT DjVu Reference Library", http://www.djvu.att.com/open/

[9]. S.Tsekeridou and I.Pitas, "Embedding Self-Similar Watermarks in the Wavelet Domain ", in Proc. of 2000 IEEE Int. Conf. on Acoustics, Systems and Signal Processing (ICASSP'00), vol. 4, pp. 1967-1970, Istanbul, Turkey, 5-9 June 2000

[10]. V.Solachidis and I.Pitas, "Self-similar ring shaped watermark embedding in 2-D DFT domain", in CD-ROM Proc. of 2000 European Signal Processing Conf. (EUSIPCO'00), Tampere, Finland, 5-8 September 2000